CrystEngComm

Accepted Manuscript

ROYAL SOCIETY OF CHEMISTRY

www.rsc.org/crystengcomm

Cite this: DOI: 10.1039/c0xx00000x

www.rsc.org/xxxxxx

Highlight

Recent Advances in the Design Strategies for Porphyrin-based Coordination Polymers

Quanzheng Zha, Xing Rui, Tiantian Wei and Yongshu Xie*

Received (in XXX, XXX) Xth XXXXXXXXX 20XX, Accepted Xth XXXXXXXXX 20XX
DOI: 10.1039/b000000x

Porphyrin-based coordination polymers (PCPs) have been investigated for a variety of applications including hydrogen storage, molecular sorption and sensing, photonics, and heterogeneous catalysis. The design and construction of functional PCPs with intriguing structures and promising properties are significant challenges for porphyrin and coordination chemists, accompanying with huge opportunities. This highlight is focused on recent advances in the design strategies for PCPs, which are summarized as following: i) introducing novel multimetal nodes such as multinuclear lanthanides and Zr_6 clusters, or inserting active metal ions into the porphyrin core; ii) design and syntheses of novel porphyrinic ligands with multi-carboxyl or pyridyl coordination sites; iii) combination with inorganic polyoxometalates; iv) encapsulation of porphyrins into the cages and post-synthetic modification.

Introduction

Structurally diverse and functionally intriguing coordination polymers (CPs) have been emerging as an attractive research topic in the fields of crystal engineering, solid-state chemistry, and materials science.[1] CPs are usually synthesized by the self-assembly of metal ions or metal clusters (nodes) with ligands (linkers), driven by metal-ligand coordination bonds that extend the structures into one, two or three dimensions. Because of the rich variety of metal species, ligands, and guests inside the pores, an enormous number of CPs have been synthesized and reported,[2] and they are promising for applications in catalysis,[3] separation,[4] gas storage[5] and molecular recognition.[6]

Multidentate chelating and bridging organic ligands with suitably disposed coordinating atoms have been extensively employed for the syntheses of CPs.[7] Macrocyclic porphyrin structures exist in many biological systems (light harvesting, oxygen transportation, and catalysis, *et al.*) with various functions.[8] And supra-molecular chemistry based on porphyrins has attracted widespread interest nowadays.[9-13]

The porphyrin core may coordinate with a metal ion, with the axial positions left for further coordination. Additionally, various coordinating moieties can be rationally introduced to the porphyrin peripheral positions. These diverse designing elements can be employed to develop multidentate chelating and bridging ligands for the construction of porphyrin-based coordination polymers (PCPs) with diverse structures and intriguing properties, which can be applied in hydrogen storage,[10] molecular sorption and sensing,[11] photonics,[12] and heterogeneous catalysis.[13] In this highlight, we will give a short review on recent advances in PCPs, mainly about the design strategies for the construction of PCPs, involving coordination with novel multimetal nodes, syntheses of new porphyrin-based ligands, combination with inorganic polyoxometalates, encapsulation of porphyrins into cages and post-synthetic modification strategies.

Strategy 1: Coordination with novel multimetal species or active metal centers

Tetrakis(4-carboxyphenyl)porphyrin (H_2TCPP) and *tetrakis*(4-pyridyl)porphyrin (H_2TPyP) are two commonly used porphyrin-

Key Laboratory for Advanced Materials and Institute of Fine Chemicals, East China University of Science & Technology, Shanghai 200237, P. R. China. E-mail: yshxie@ecust.edu.cn

Yongshu Xie

Yongshu Xie received the Ph.D. degree of chemistry from Zhejiang University. Following postdoctoral experience and associate professorship in University of Science and Technology of China, he successively joined Prof. Xuming Peng group in National Taiwan University, Prof. Hiroyuki Furuta group in Kyushu University, Prof. Katsuhiko Ariga and J. P. Hill group in National Institute for Materials Science (Japan) as a research fellow. Now he is a professor in Institute of Fine Chemicals, East China University of Science and Technology. His research interests are porphyrin chemistry, functional coordination chemistry, and electronic and optical materials based on conjugated organic molecules.

based ligands (Scheme 1) for the construction of PCPs.[14] Thus, various multiporphyrin frameworks with different topologies and dimensionalities have been constructed through the coordination of their peripheral carboxyphenyl or pyridyl moieties. Meanwhile, the easy metalation of the porphyrin core provides another opportunity for coordination of two axial ligands. Thus, H_2TCPP and H_2TPyP seem to be almost inexhaustible sources for the construction of either hydrogen-bonding or coordination-driven PCPs[15]. In this section, we will make a brief description of recent advances in this respect, with emphasis on novel structures and the applications as heterogeneous catalysts.

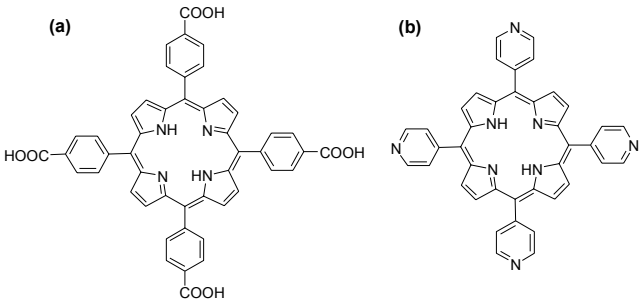

H_2TCPP H_2TPyP

Scheme 1. Chemical structures of two traditional porphyrinic ligands, H_2TCPP (a) and H_2TPyP (b).

1.1 Coordination of traditional porphyrins with multinuclear lanthanides or the Zr_6 clusters

Trivalent lanthanide ions with large radii, exhibit high coordination numbers and strong affinity for oxo ligands. Many of the acetate/oxalate salts of trivalent lanthanide ions consist of polynuclear metal ion clusters bridged by several acetate/oxalate anions,[16] making them suitable for the construction of novel PCPs. Goldberg and coworkers[17] reported the first examples of hybrid porphyrin-lanthanide coordination polymers by reactions of H_2TCPP with the Pr_2(oxalate)$_3$, Nd_2(oxalate)$_3$, and Dy_2(oxalate)$_3$ hydrated salts. As depicted in Fig. 1a , two Pr^{3+} cations are bridged by four carboxylates of four different porphyrins. These Pr_2 clusters are further interlinked to each other by bridging oxalates, thus affording a polymeric [-Pr_2-(porphyrin)-oxalate-]$_\infty$ coordination pattern. For the corresponding Dy(III) complex (Fig. 1b), the fundamental tetranuclear synthon consists of four bridged Dy ions connecting to 12 porphyrin molecules distributed between three porphyrin layers. Each of the four porphyrins of the central layer utilizes its carboxylate to bridge the two "inner" Dy ions. Porphyrin species in the first and the third layers either coordinate to the "outer" Dy ions or bridge the outer and the inner Dy atoms. These results demonstrated the effective use of the multimetallic lanthanide species in the construction of PCPs based on the tetrafunctional H_2TCPP ligand.

Recently, the Zr_6 cluster has attracted increasing attention as one of the most stable building units for the construction of MOFs. Zr^{IV} cation and carboxylate anion can be classified as the hard acid and the hard base, respectively.[18] And the high charge density (Z/r) of Zr^{IV} may polarize the carboxylic oxygens, thus affording very strong Zr-O bonds with significant covalent character,[19] making them resistant to water, base, and even acid.

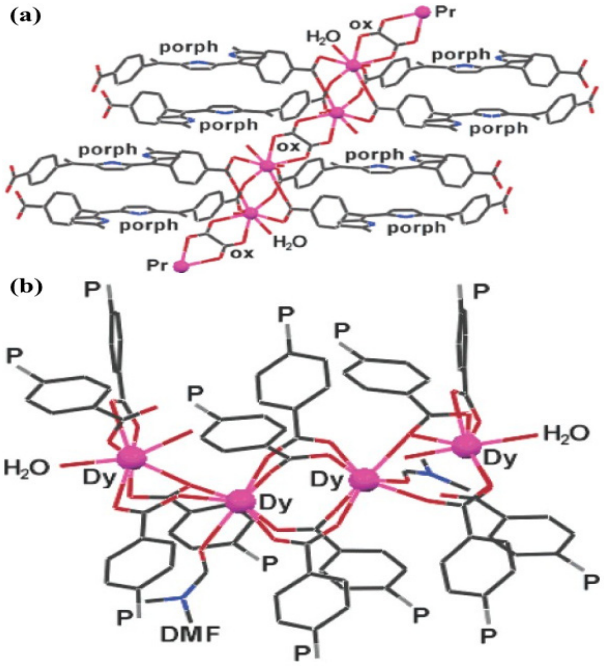

Figure 1. (a) The continuous coordination pattern of Pr_2 clusters, involving the Pr metal ions, H_2TCPP (only half of the ligand is shown at each site), and the oxalate anions (ox). (b) The tetranuclear coordination synthon, showing the binding of 12 porphyrins (organized in three layers) to four Dy ions. Only the terminal carboxyphenyl groups are shown, with "P" representing the remaining porphyrin framework. (Reproduced from ref. 17 with permission, copyright 2006 American Chemical Society.)

With elaborately selected starting materials by Hongcai Zhou and coworkers,[20] solvothermal reactions of Fe-TCPP, $ZrCl_4$ and benzoic acid in N,N-diethylformamide (DEF) for 48 h at 120 °C yielded crystals of PCN-222(Fe) (PCN represents porous coordination network), with a framework consisting of the square planar porphyrin ligands connected to Zr_6 clusters. Each Fe-TCPP moiety coordinates to four 8-connected Zr_6 clusters with a twisted

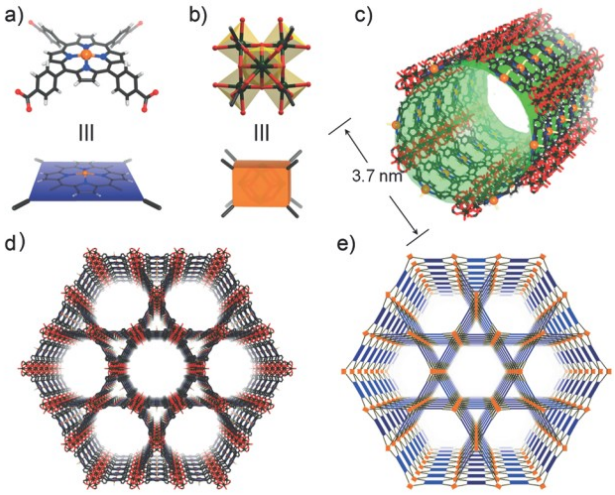

Figure 2. Crystal structure and underlying network topology of PCN-222(Fe). The Fe-TCPP (a; blue square) is connected to four 8-connected Zr_6 clusters (b; light orange cuboid) to generate a 3D network in Kagome-like topology (d, e) with 1D large channels (c; green pillar). Zr black spheres, C gray, O red, N blue, Fe orange. H atoms were omitted for clarity. (Reproduced from ref. 20 with permission, copyright 2012 John Wiley and Sons.)

angle, forming a 3D network with Kagome-like topology (Fig. 2). Remarkably, the framework shows mesoporosity containing large 1D hexagonal open channels with a large diameter of 3.7 nm, ranking among the largest ones for MOFs.[21,22] And the framework survived even after immersion in concentrated HCl, which has been rarely observed for MOF materials. In addition, PCN-222(Fe) exhibited bio-mimetic catalytic activity for a variety of oxidation reactions, due to the presence of the active porphyrin centers and large open channels.

Solvothermal reactions of $ZrCl_4$, H_2TCPP, acetic acid, and benzoic acid in DEF at 120 °C yielded single crystals of PCN-225.[23] Two kinds of crystallographically independent Zr atoms are observed and both are coordinated to eight oxygen atoms as depicted in Fig. 3. Six Zr atoms coordinate with eight μ_3-oxygen atoms to afford a cluster with a $Zr_6(\mu_3\text{-}O)_4(\mu_3\text{-}OH)_4$ core. And each $TCPP^{2-}$ ligand is linked to four such Zr_6 clusters, thus generating a 3D porous structure with a (4, 8)-connected *sqc* net structure. PCN-225 also demonstrated exceptional chemical stability. The framework remains intact in aqueous solutions within the pH range of 1 to 11, and this is the broadest pH range that PCPs can survive thus far. Furthermore, the central core region of the porphyrin free base demonstrated protonation-deprotonation equilibria, resulting in pH dependent fluorescence intensity. Interestingly, 7~10 is the most sensitive pH range for the intensity response, indicating that PCN-225 is promising for pH sensing, especially in the neutral to weakly basic pH range.

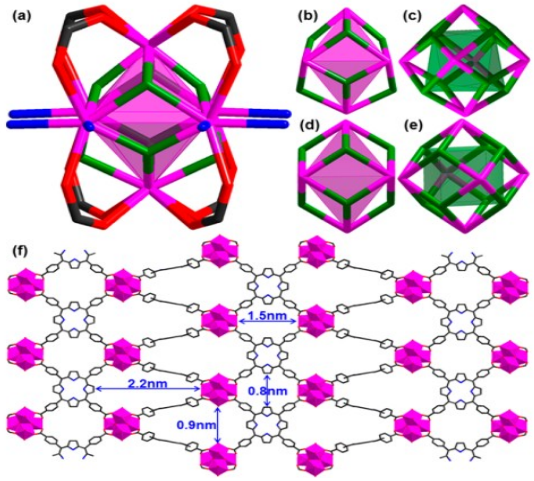

Figure 3. (a) $Zr_6(\mu3\text{-}O)_4(\mu3\text{-}OH)_4(OH)_4(H_2O)_4(COO)_8$ cluster. The oxygen atoms from μ3-OH/-O, -OH/H_2O and -COO groups are shown in green, blue and red, respectively; (b, c) Irregular $Zr_6(\mu3\text{-}O)_4(\mu3\text{-}OH)_4$ cluster core in PCN-225, in which six Zr atoms combine an octahedron shaded in pink (b) whereas eight μ_3 oxygen atoms form a highly distorted polyhedron highlighted in green (c). (d, e) Idealized $Zr_6(\mu3\text{-}OH)_8$ cluster core in PCN-222, where the Zr_6 octahedron and $(\mu3\text{-}O)_8$ cube are drawn in pink and green, respectively; and (f) View of the structure of PCN-225 along the b axis with two types of channels. The Zr, O, C, N atoms are shown in pink, red, gray and blue, respectively. H atoms are omitted for clarity. (Reproduced from ref. 23 with permission, copyright 2013 American Chemical Society.)

By carefully varying the ratio of the starting materials and the reagents, a series of new porous porphyrinic zirconium MOFs (denoted as PCN-224) were obtained.[24] Different from the 12 connected Zr_6 cluster observed in the UiO-66[25] and 8 connected Zr_6 cluster in PCN-222, only six edges of the Zr_6 octahedron are bridged by carboxylates from the $TCPP^{2-}$ ligands in PCN-224. By using triple amount of $ZrCl_4$ as that for the synthesis of PCN-222, more Zr atoms would compete with each other to coordinate with $TCPP^{2-}$. Eventually, the increased Zr-TCPP ratio led to the lower connectivity on the Zr_6 cluster and the cluster symmetry was reduced to D_{3d}. With the reduced number of carboxylate linkers, PCN-224 contains more free space to generate the 3D open channels (Fig. 4) with a very high BET surface area of 2600 $m^2 \cdot g^{-1}$. It also showed remarkable stability in aqueous solutions within a wide pH range. Moreover, the framework containing Co atoms in the porphyrin centers was observed to be a reusable heterogeneous catalyst for CO_2 epoxide coupling reactions.

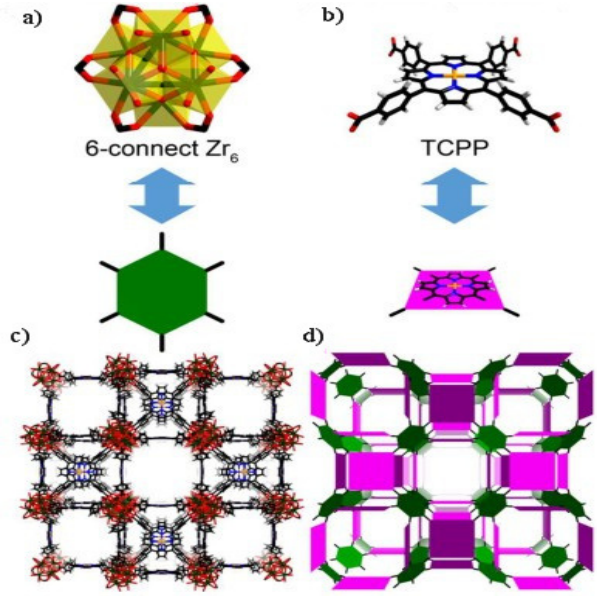

Figure 4. The 6-connected D_{3d} symmetric Zr_6 (a) in PCN-224 and tetratopic TCPP ligands (b) with twisted dihedral angles generate a framework with 3D nanochannels (c, d). Colour scheme: Zr, green spheres; C, grey; O, red; N, blue; Ni, orange; and H, white. (Reproduced from ref. 24 with permission, copyright 2013 American Chemical Society.)

1.2 Inserting active metal ions into the porphyrin core

Pd^{II}-porphyrin has been demonstrated to be a catalytically active building block for construction of functional MOFs by Chuande Wu *et al*.[26] A mixture of Pd-TCPP and $Cd(NO_3)_2{\cdot}4H_2O$ in DMF, MeOH and acetic acid at 80 °C for ten days yielded crystals of $[Cd_{1.25}(Pd\text{-}H_{1.5}TCPP)(H_2O)]{\cdot}2DMF$. This solid incorporates the functional porphyrin ligand with active Pd^{II} sites occurring in the porous framework. Each Pd-TCPP ligand acts as an octadentate ligand to coordinate with eight Cd atoms from four neighboring Cd chains, assembling into a 3D framework structure (Fig. 5) which contains two kinds of channels with dimensions of 4.61 × 12.55 $Å^2$ and 8.27 × 9.32 $Å^2$ (considering the van der Waals diameters) along the *a* axis. The frameworks remain intact upon removing the solvents or exchanging them with other guests, demonstrating its good framework stability. Moreover, the solid shows significant styrene oxidation activity with the advantages of easy separation and good recyclability.

Sn^{IV}-porphyrins, with good photochemical characteristics for light activation, are easily deactivated by reaction with the singlet oxygen atoms. A typical solution to this problem is to immobilize these photoactive sites in the channel walls of porous MOFs[27] to realize good photocatalytic performance in heterogeneous phases.

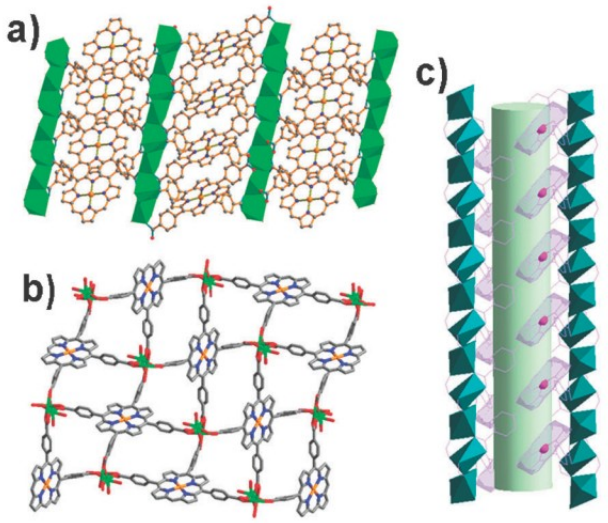

Figure 5. (a) A view of the 3D framework down the [110] direction, showing the arrangement of the palladium-porphyrins; (b) The 3D framework viewed along the *a* axis, showing the 1D open channels and the accessible Pd^{II} sites; and (c) Side view of the 1D channel in the porous framework. (Reproduced from ref. 26 with permission from The Royal Society of Chemistry.)

A 3D porous MOF of $[Zn_2(H_2O)_4Sn^{IV}(TPyP)(HCOO)_2]\cdot 4NO_3\cdot DMF\cdot 4H_2O$[28] was synthesized by heating a mixture of $Sn^{IV}(OH)_2TPyP$ and $Zn(NO_3)_2\cdot 6H_2O$ in DMF and CH_2Cl_2 at 50 °C for five days. Each Sn^{IV}-TPyP ligand coordinates with four Zn atoms to afford a 2D framework structure. And the lamellae extend into a 3D porous network through the connection between the formates and the tin atoms in the porphyrin cores (Fig. 6). It demonstrates remarkable photocatalytic activities for the oxygenation of phenol and sulfides under Xe lamp irradiation with excellent yields and selectivity in heterogeneous phases.

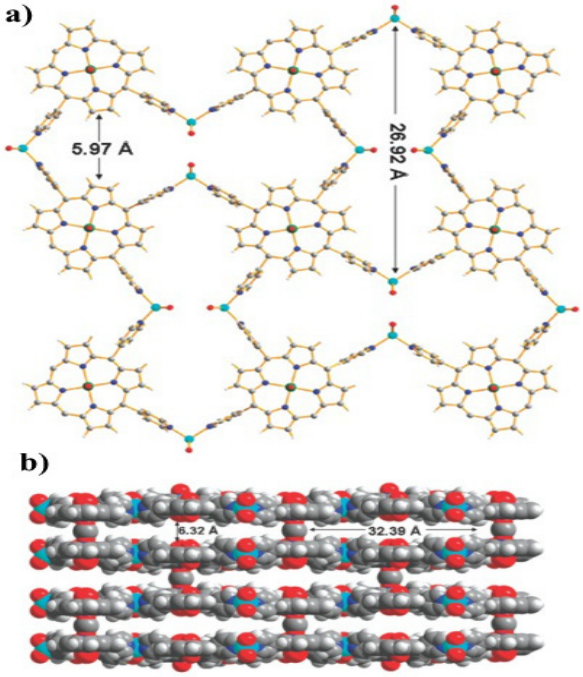

Figure 6. (a) The lamellar network of Zn^{II} atoms linking up Sn^{IV}-porphyrins as viewed along the *c* axis; and (b) A side view of the 3D network of the lamellae linked by the formate struts along the b axis. (Reproduced from ref. 28 with permission, copyright 2011 American Chemical Society.)

Israel Goldberg *et al.* reported the coordination of six-coordinate Sn-TPyP moiety with multidentate carboxylic acids used as axial ligands.[29] Five new $Sn(acid)_2$-TPyP complexes were obtained with the networks sustained by extensive hydrogen bonds between the axial acid ligands (proton donors) and the pyridyl N-sites of the porphyrin (proton acceptors). Combination with different acid ligands results in different connectivity features of these five supramolecular assemblies (Fig. 7). When 5-hydroxy-isophthalic acid and trimesic acid ligands were used, the resulting structures present 1D hydrogen-bonded chains only, as solvation effects prevent interporphyrin interaction in other directions. The combination with 5-amino-isophthalic acid afforded a 2D hydrogen-bonding network, while the reaction with cis-1,3,5-cyclohexane-tricarboxylic acid and 5-bromo-isophthalic acid generated 3D interlinked assemblies.

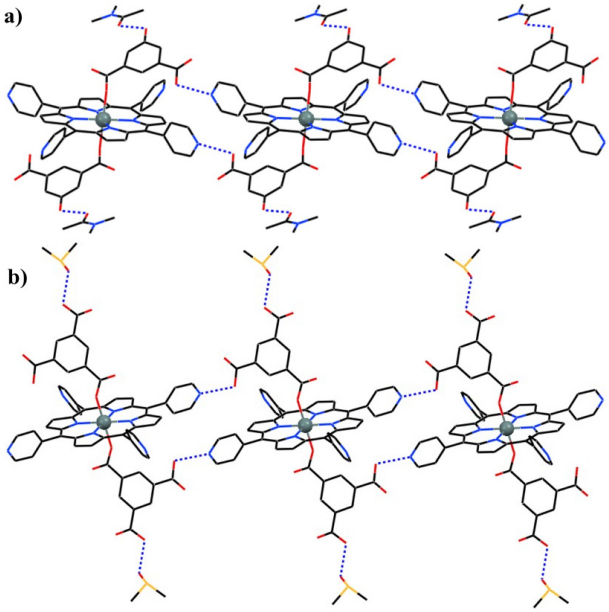

Figure 7. Self-assembly of the $[Sn\text{-}TPyP(A^-)_2]$ units into 1D hydrogen bonded chains (depicted by dotted lines). Note that the additional hydrogen bonding sites on the axial ligands (OH and COOH) are engaged in hydrogen bonds to the DMA and DMSO solvent moieties, respectively. (Reproduced from ref. 29 with permission, copyright 2013 American Chemical Society.)

Strategy 2: Coordination of novel porphyrin-based ligands

The design and syntheses of novel porphyrin-based ligands are promising for creating coordination assemblies with novel structures and intriguing properties. Typical porphyrinic ligands recently developed for the construction of PCPs are depicted in Scheme 2. It is noteworthy that the PCPs listed in this section were constructed from only two components, a porphyrinic linker together with discrete metal nodes, without using pillar ligands such as 4,4'-bipyridine,[30-42] thus leaving the noncoordinated axial positions of the metal centers in the porphyrin cores as active metal sites.

2.1 H_2T^3CPP and H_2T^3PyP with chair- and table-like orientational versatility

Following the rich supramolecular chemistry of H_2TCPP and H_2TPyP, *tetrakis*(3-carboxyphenyl)porphyrin (H_2T^3CPP) and

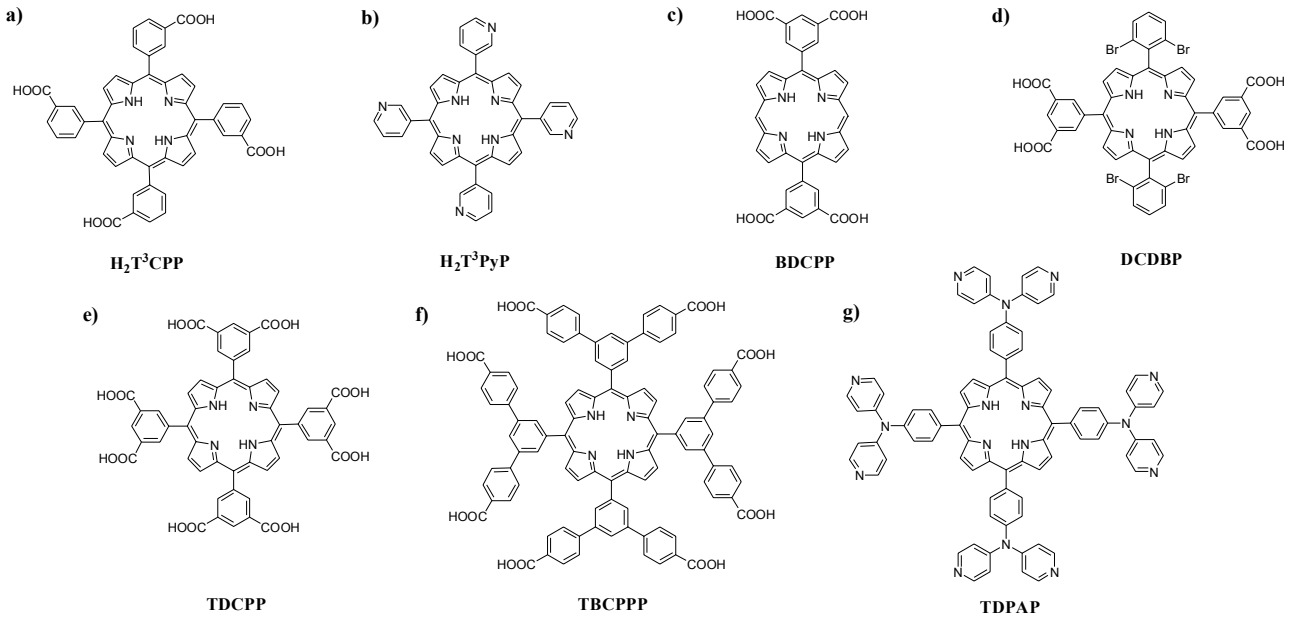

Scheme 2. Chemical structures of recently developed porphyrin ligands. (a) H_2T^3CPP, (b) H_2T^3PyP, (c) BDCPP, (d) DCDBP, (e) TDCPP, (f) TBCPPP, (g) TDPAP.

tetrakis(3-pyridyl)porphyrin (H_2T^3PyP) (Scheme 2a, 2b) have also been demonstrated to form intriguing coordination structures.[30-32] Because the four 3-carboxyphenyl or 3-pyridyl arms of the two ligands can assume alternative orientations, positioned either above or below the porphyrin macrocycle, leading to the orientational versatility of chair- and table-like conformers (Scheme 3). In the "chair" conformer, two adjacent carboxylic moieties are oriented upward and the other two downward, while in the "table" isomer, all four carboxylic arms are oriented in the same direction.

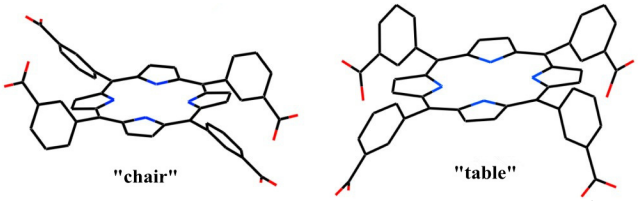

Scheme 3. Illustrations of the chair- and table-like conformers of the H_2T^3CPP scaffold differing in relative orientations of the carboxyphenyl "legs". (Reproduced from ref. 30 with permission, copyright 2013 American Chemical Society.)

Solvothermal reactions of H_2T^3CPP with Cd^{2+} or Zn^{2+} ions can afford a molecular-box in which two table-like Cd-T^3CPP moieties are linked by four Cd ions (Fig. 8), as well as other coordination polymers of 1D and 2D connectivity.[30] Hydrogen-bonded networks between the chair-like H_2T^3CPP/Co-T^3CPP moieties and various amine ligands were also obtained. While the occurrence of the "table" conformer of H_2T^3CPP has been observed for the first time, new supramolecular materials are expected to emerge in the future. These results indicate that the H_2T^3CPP scaffold can be effectively used to construct various PCPs through direct multiple-coordination, as well as extended hydrogen-bonding networks.

Similar to H_2T^3CPP, H_2T^3PyP also have attracted extensive attention in recent years. Choe[31] reported a H_2T^3PyP-based coordination polymer (MPF-3), with a 2D interdigitated framework similar to the Cairo pentagonal tessellation. Goldberg[32] expanded the library of the H_2T^3PyP-based coordination networks assembled through either endocyclic or exocyclic metal ion linkers, demonstrating the utility of this ligand in the construction of 2D and 3D PCPs. It is obvious that the conformational versatility of H_2T^3CPP and H_2T^3PyP enriches the coordination architectures of this scaffold, providing a better choice for the design of novel PCPs.

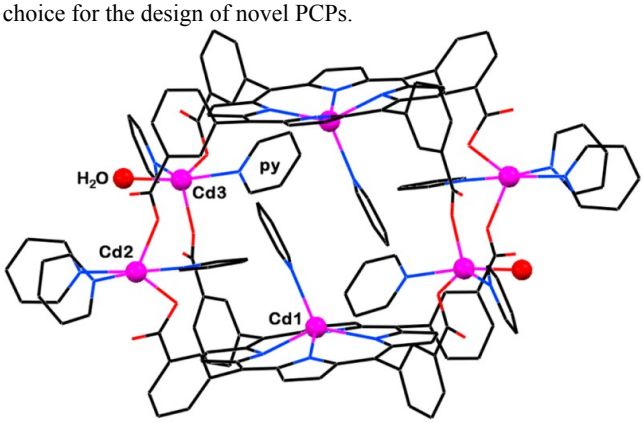

Figure 8. The discrete (0-D) molecular-box-type coordination assembly that involves two table conformers of Cd-T^3CPP tessellated into a box-type dimer by four (COO^-)-Cd-(COO^-) coordination bridges. (Reproduced from ref. 30 with permission, copyright 2013 American Chemical Society.)

2.2 BDCPP and DCDBP with a pair of isophthalates

The disposition of the coordinating atoms may be changed for the purpose of developing novel PCPs. Ma *et al.*[33] reported a porphyrin ligand, 5,15-bis(3,5-dicarboxyphenyl)porphyrin (BDCPP, Scheme 2c), in which two isophthalates are introduced, for the construction of a confined nanoscopic polyhedral cage-containing metal-metalloporphyrin framework (MMPF-1) *via* the reaction of BDCPP with $Cu(NO_3)_2$ in dimethylacetamide (DMA)

at 85 ℃. As shown in Fig. 9, Sixteen BDCPP ligands are connected with eight paddlewheel second building units (SBUs) to afford a nanoscopic cage: four dicopper paddlewheel SBUs are linked by four isophthalate moieties from four BDCPP ligands to form the top of the cage; they are pillared to four dicopper paddlewheel SBUs at the bottom of the cage through eight BDCPP ligands. The irregular rhombicuboctahedron cage contains a high density of 16 open Cu sites, and such cages adopt a "ABAB" packing mode, thus constricting its pore size, which facilitates selective adsorption of H_2 and O_2 over N_2, and CO_2 over CH_4.

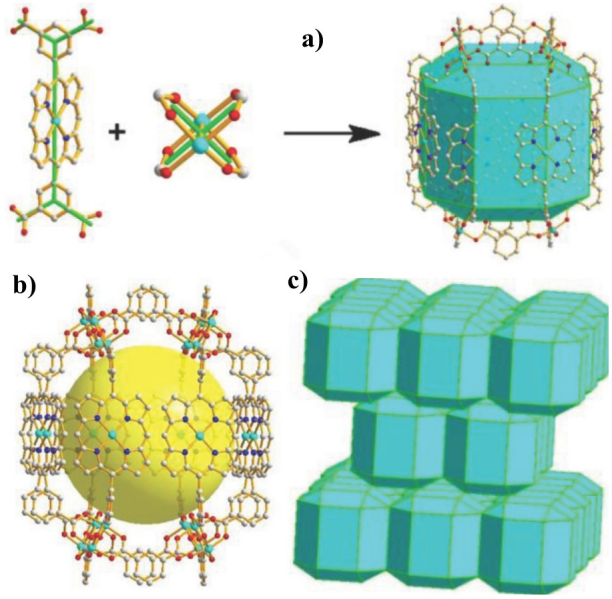

Figure 9. (a) Illustration of linking BDCPP ligand and dicopper paddlewheel to form the irregular rhombicuboctahedral cage; (b) Nanoscopic cage enclosed by eight dicopper paddlewheel SBUs and 16 BDCPP ligands (eight are face-on porphyrins, and the other eight only provide isophthalate units); and (c) "ABAB" packing of rhombicuboctahedron layers in MMPF-1. (Reproduced from ref. 33 with permission, copyright 2011 American Chemical Society.)

Mori *et al*.[34] also investigated the BDCPP ligand, however, they firstly synthesized the building blocks of M-BDCPP [M =Zn^{2+}, Ni^{2+}, Pd^{2+}, $Mn^{3+}Cl$, $Ru^{2+}(CO)$], and then the reaction of $Cu(NO_3)_2{\cdot}3H_2O$ with M-BDCPP gave five PCPs ([Cu_2(M-BDCPP)] series), which are isostructural regardless of the identity of the central metal in the porphyrin core. There is an internal spherical cavity of *ca.* 20 Å in diameter (the Zn-Zn and Cu-Cu distances between the opposite positions are 20.3 Å and 19.6 Å, respectively) in the 3D porous structure of these PCPs, which is surrounded by 16 accessible metal sites (Fig. 10). Impressively, accessible metal sites can be systematically incorporated into the framework without changing the framework topology in this case. The [Cu_2(M-BDCPP)] series also exhibit permanent porosity and good N_2 and H_2 adsorption properties.

A similar ligand, 5,15-bis(3,5-dicarboxyphenyl)-10,20-bis(2,6-dibromophenyl)porphyrin (DCDBP, Scheme 2d) was reported by Ma *et al*.[35] MMPF-3 was prepared solvothermally from DCDBP and $Co(NO_3)_2$, and it can be used as a polyhedral cage-based nanoreactor exhibiting a high density of five catalytically active cobalt centers per nm^3. There are three types of polyhedral cages in MMPF-3, i.e., cubohemioctahedron, truncated tetrahedron and

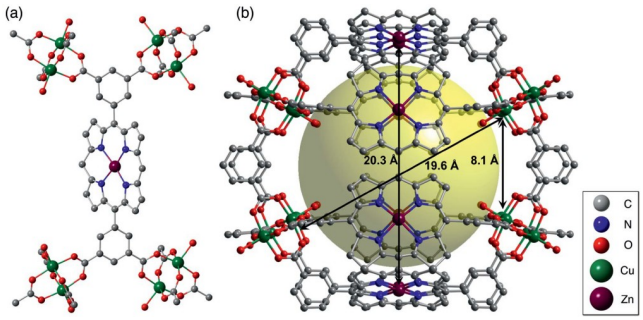

Figure 10. (a) Zn-BDCPP moiety of [Cu_2(Zn-BDCPP)]; and (b) cage consisting of eight Zn-BDCPP ligands and eight paddlewheel Cu_2 nodes. H atoms are omitted for clarity. (Reproduced from ref. 34 with permission, copyright 2012 John Wiley and Sons.)

truncated octahedron, which are interconnected to form a 3D structure (Fig. 11), exhibiting permanent microporosity confirmed by CO_2 adsorption. Due to the high density of active cobalt centers and the porous structure, MMPF-3 demonstrates good performance in catalytic epoxidation of trans-stilbene regarding both selectivity and overall conversion, indicating that the construction of polyhedral cage-based nanoreactors with a high density of catalytically active metal centers is a useful approach for developing new PCPs as highly efficient heterogeneous catalysts.

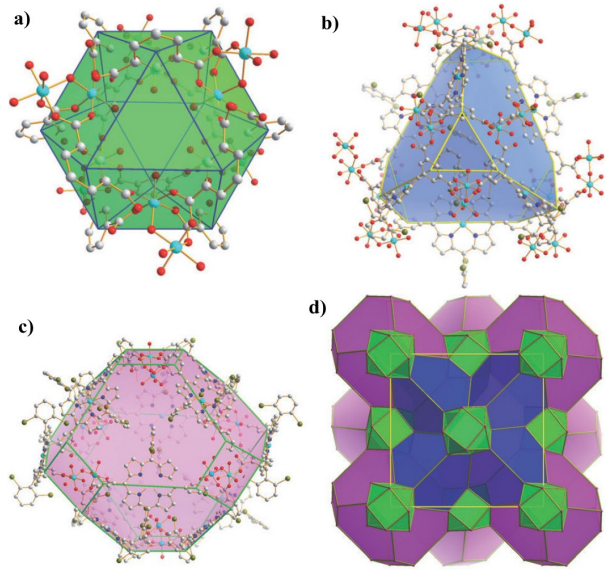

Figure 11. The three types of polyhedral cages present in MMPF-3: a) cubohemioctahedron, b) truncated tetrahedron, and c) truncated octahedron. d) 3D structure of MMPF-3 illustrating how its polyhedral cages are connected. (Reproduced from ref. 35 with permission, copyright 2012 John Wiley and Sons.)

2.3 TDCPP and TBCPPP: Innovative octatopic porphyrin ligands

For the purpose of designing novel PCPs based on porphyrin ligands with the abilities to coordinate with more metal centers, more than four carboxylic or pyridyl moieties may be introduced. In this respect, a new octatopic porphyrin ligand, 5,10,15,20-tetrakis(3,5-biscarboxyl-phenyl)porphyrin (TDCPP, Scheme 2e),

has been widely investigated by Chuande Wu[36] and Shengqian Ma *et al*.[37, 39, 40] Wu and coworkers used TDCPP to construct three porous metalloporphyrinic frameworks (ZJU-18, ZJU-19, and ZJU-20),[36] whose structures are 3-periodic, binodal, edge-transitive nets with the Reticular Chemistry Structure Resource symbol of **tbo** (Fig. 12), showing intercrossed pore windows of about 11.5 Å and pore cages of about 21.3 Å in diameter. These three isostructural MOFs were synthesized by heating a mixture of M-TDCPP (M = $Mn^{III}Cl$ or Ni^{II}) and $MnCl_2$ or $CdCl_2$ in a mixed solvent of DMF and acetic acid at 80 °C for one week. Remarkably, ZJU-18 exhibits highly effcient and selective oxidation of ethylbenzene to acetophenone in an almost quantitative yield and a turnover number of 8076 after 48 h. However, the conversion decreases with the increasing size of the substrates. The much lower catalytic conversion for the larger substrates might be attributed to their diffcult access to the interior pores of ZJU-18, so the catalytic reaction mainly occurs on the exterior surfaces.

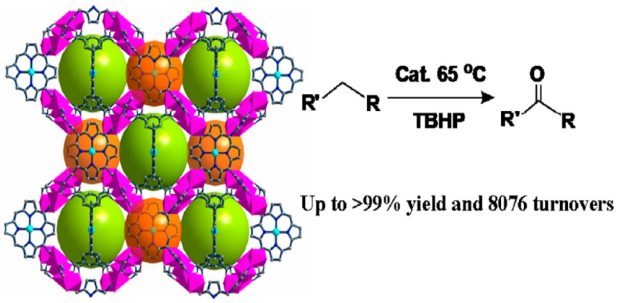

Figure 12. The porous 3D crystal structure of ZJU-18. It exhibits highly effcient and selective oxidation of ethylbenzene to acetophenone. (Reproduced from ref. 36 with permission, copyright 2012 American Chemical Society.)

TDCPP was also used for the reaction with $Co(NO_3)_2{\cdot}6H_2O$ in DMA to construct a novel (6,8,8)-connected MOF, MMPF-2,[37] which contains a rare distorted cobalt trigonal prism SBU, in which three cobalt atoms are bridged by a μ_3-OH and six carboxylate groups from six TDCPP ligands (Fig. 13). For the porphyrin ligand, four carboxylates point upwards and the other four point downwards, thus affording a ''face-to-face'' configuration of the porphyrin macrocycles. MMPF-2 possesses permanent microporosity with a high surface area of 2037 $m^2{\cdot}g^{-1}$. In addition, high density of open cobalt centers was observed in the channel walls formed by the ''face-to-face'' configuration, resulting in excellent CO_2 capture performance with an uptake capacity of 170 $cm^3{\cdot}g^{-1}$ at 273 K and 1 bar.

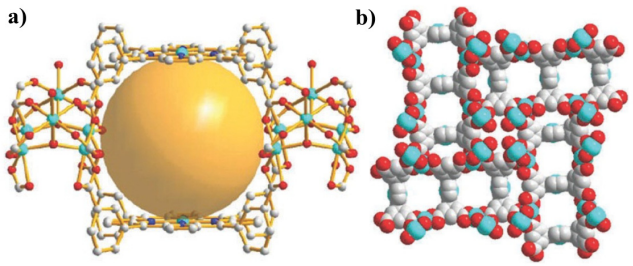

Figure 13. (a) Three cobalt porphyrins located in the ''face-to-face'' configuration in MMPF-2; and (b) space filling model of three types of channels in MMPF-2 viewed from the *c* direction. (Reproduced from ref. 37 with permission from The Royal Society of Chemistry.)

Metal-organic materials constructed from polyhedral supermolecular building blocks (SBBs) can offer exquisite control over the structures and afford useful features such as multiple cage types and relatively narrow pores.[38] Thus, MMPF-4 (M = Zn) and MMPF-5 (M = Cd)[39] were prepared by solvothermal reactions of TDCPP with $Zn(NO_3)_2$ and $Cd(NO_3)_2$ respectively in DMSO at 135 °C. Fig. 14 illustrates how one face of each TDCPP moiety is metallated with Zn (II) *in situ*. In the context of the SBB, Zn-TDCPP serves as a 4-connected node that is connected with triangular paddlewheel $Zn_2(CO_2)_3$ moieties, constructing a small cubicuboctahedron composed of the faces of six Zn-TDCPP moieties linked by eight $Zn_2(CO_2)_3$ units. The resulting cubicuboctahedral SBBs are the first uniform polyhedral SBBs based on porphyrin blocks. The high symmetry augmented *pcu* topology networks of MMPF-4 and MMPF-5, exhibit two distinct polyhedral cages and are permanently microporous with selective CO_2 uptake.

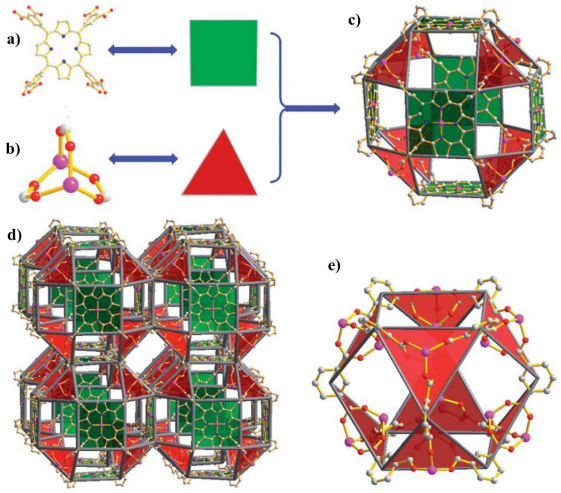

Figure 14. (a) TDCPP serves as a square molecular building block (MBB); (b) $Zn_2(CO_2)_3$ paddlewheel moiety serves as a triangular MBB; (c) the small cubicuboctahedron in MMPF-4 is formed by 6 square Zn–TDCPP MBBs and 8 triangular $Zn_2(CO_2)_3$ MBBs; (d) Zn–TDCPP ligands fuse the square faces of small cubicuboctahedra to afford an augmented *pcu* network with two types of cavity in MMPF-4; and (e) the cage formed between the SBBs can be described as octahemioctahedron with an internal diameter of 11.189 Å and window dimensions of 8.048 Å × 8.048 Å (atom to atom distance). (Reproduced from ref. 39 with permission from The Royal Society of Chemistry.)

In the structure of MMPF-5, the Cd^{II} cation residing within the porphyrin core of TDCPP lies far out of the porphyrin plane, indicative of weak coordination of Cd^{II}. These results prompted Ma *et al*.[40] to exchange the large Cd^{II} cation with smaller active divalent metal cations. Immersing the crystals of MMPF-5 in the DMSO solution of $Co(NO_3)_2$ at 85 °C for two days afforded the Co^{II}-exchanged MMPF-5(Co). Crystal structure, UV/Vis and ICP-MS studies confirmed the complete replacement of Cd^{II} with Co^{II} occurring exclusively within the porphyrin macrocycles, while the Cd^{II} cations in the framework remain intact, possibly due to their strong chelation with six carboxylate oxygen atoms. Therefore the small cubicuboctahedral cage in MMPF-5(Co) features the faces of six Co^{II}-metalated TDCPP moieties that are linked by eight triangular $Cd(CO_2)_3$ moieties. MMPF-5(Co) demonstrated interesting performance in catalytic epoxidation of

trans-stilbene. All these findings suggest an easy and versatile method to create PCPs containing different active centers within the same framework structure for heterogeneous catalysis.

Jian Zhang and coworkers[41] designed a new octatopic porphyrin, *tetrakis*{3,5-bis[(4-carboxy)phenyl]phenyl}porphyrin (TBCPPP, Scheme 2f), by inserting a phenyl group between each carboxyl group and the corresponding meso-phenyl ring in the TDCPP molecule, in order to increase the rotational flexibility of the carboxyphenyl groups. With this modified ligand, a "pillar-free", highly porous metalloporphyrinic framework $\{[Zn_2(H_2O)_2]_2[(Zn\text{-}TBCPPP)(H_2O)_2]\}_n$ (UNLPF-1), was generated *via* solvothermal reaction of TBCPPP and $Zn(NO_3)_2{\cdot}6H_2O$ in DMF and acetic acid (30:1, v/v) at 80 °C for 72 h. UNLPF-1 possesses a common type of SBU, namely, square paddlewheel $[Zn_2(COO)_4(H_2O)_2]$. Each SBU links four TBCPPP ligands and each TBCPPP ligand links eight *in situ* generated SBUs (four above and four below the porphyrin plane) to afford a 3D non-interpenetrated structure (Fig. 15). Two adjacent porphyrin macrocycles, together with four paddlewheel SBUs, form a cage with large dimensions of 14.5 Å × 23.7 Å (measured between the proximal Zn centers and the two diagonal SBUs). Impressively, UNLPF-1 exhibits high CO_2 adsorption capacity and selectivity for CO_2 over N_2.

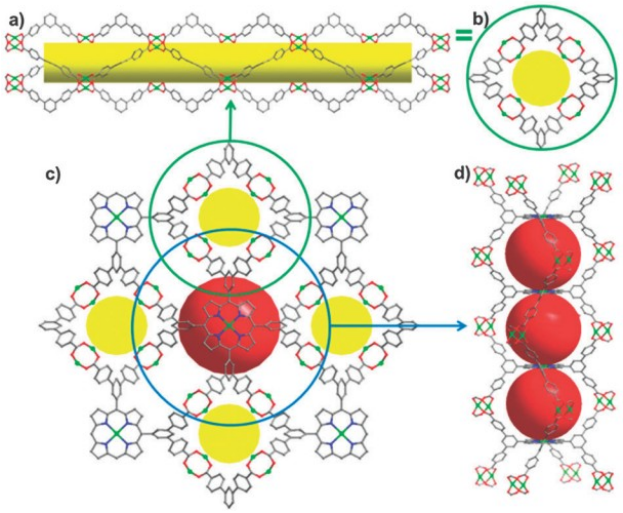

Figure 15. Side view (a) and top view (b) of a single square-shaped tubular supramolecular building block; (c) 3D network connectivity along the [001] direction between the paddlewheels and the V-shaped terphenyl arms connecting with the porphyrin linker; and (d) side view of the 1D eclipsed packing of the porphyrins (cages are represented by red spheres). (Reproduced from ref. 41 with permission from The Royal Society of Chemistry.)

2.4 TDPAP containing four 4,4'-dipyridylamine moieties

Recently, the Xie Group designed and synthesized a novel porphyrin ligand, 5, 10, 15, 20-tetrakis(4,4-dipyridylamino-phenylene)porphyrin (TDPAP, Scheme 2g), by introducing four 4,4'-dipyridylamine moieties to a porphyrin platform.[42] The TDPAP ligand can coordinate with 4-7 metal centers (Scheme 4) using its multiple peripheral pyridines and the porphyrin core, resulting in a rich structural diversity: a hydrogen-bonded 1D chains linked by $[(H_2O)_2Cl_2]^{2-}$ moieties, a 3D structure formed by the π···π stacking interactions between interpenetrated 2D networks, a 2D structure with large cavities composed of 50- and 70-membered metallomacrocycles (Fig. 16), a complicated 2D structure linked by zigzag chains, and a stairlike 2D structure

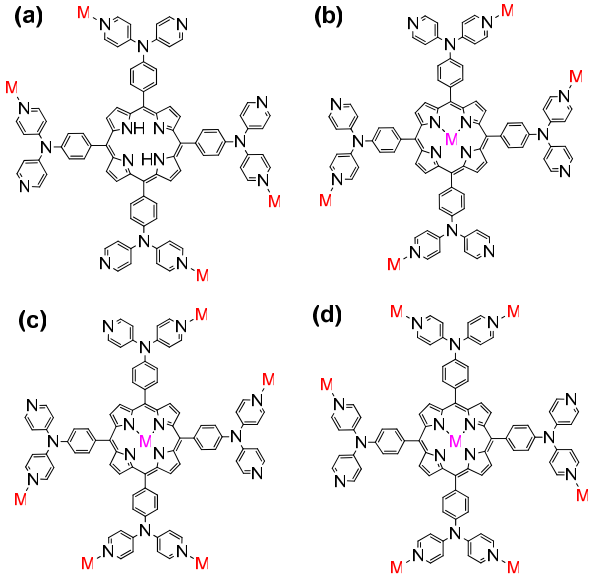

Scheme 4. The demonstrated coordination modes of TDPAP. (Reproduced from ref. 42 with permission, copyright 2013 American Chemical Society.)

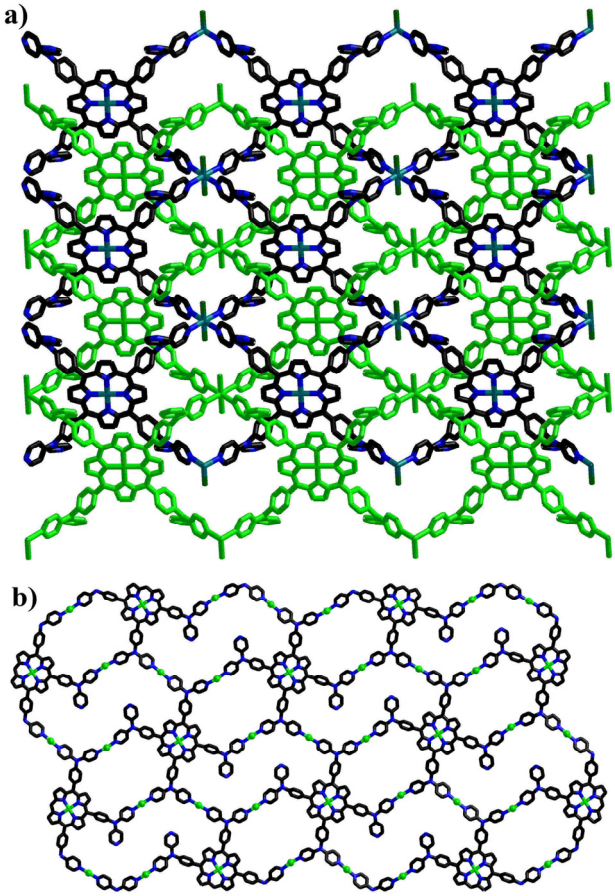

Figure 16. (a) The interpenetrated 2D coordination networks constructed by TDPAP and $MnCl_2$; and (b) The 2D network composed of 50- and 70-membered metallo-macrocycles, constructed from TDPAP and $Cu(OAc)_2$. (Reproduced from ref. 42 with permission, copyright 2013 American Chemical Society.)

containing binuclear $[Cd_2(CO_2)_4]$ subunits. The 4,4'-dipyridylaminophenylene moieties may rotate around the porphyrin framework, resulting in good conformational flexibility of the TDPAP ligand.

Strategy 3: Insertion of polyoxometalates

Polyoxometalates (POMs) are negatively charged metal-oxide clusters with oxo-rich surfaces and controllable shape and size.[43] POMs represent a remarkable class of molecular building blocks for the construction of inorganic-organic hybrid materials which has become a rapidly growing area.[44] Bearing abundant oxygen donors on the surface, POMs are ideal inorganic components to construct hybrid materials with diverse composition and unique properties. In the past decades, such types of inorganic-organic hybrid materials have been applied in catalysis, materials science, and pharmaceutics.[45] Hence, it is appealing to assemble novel coordination polymers by the integration of porphyrin-based organic ligands, transition-metal complex moieties and POMs.

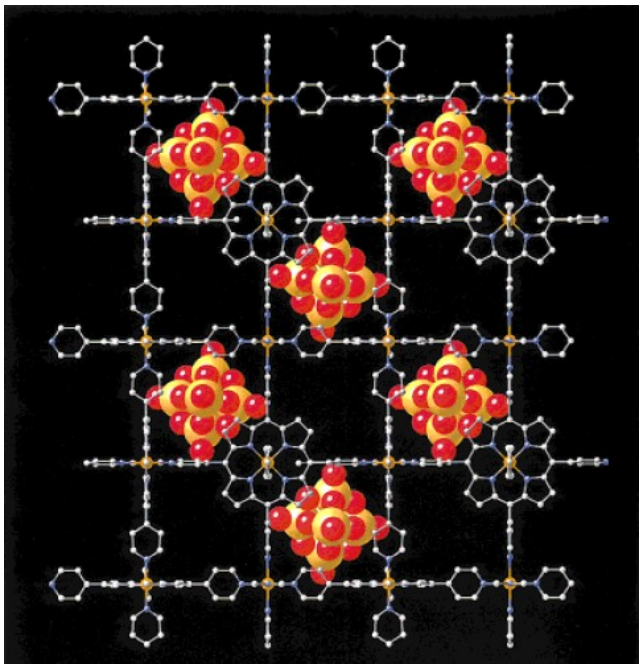

Figure 17. A view of the structure of $[\{Fe(TPyP)\}_3Fe(Mo_6O_{19})_2]\cdot xH_2O$ parallel to the crystallographic *c* axis. (Reproduced from ref. 46 with permission, copyright 1999 John Wiley and Sons.)

Zubieta and co-workers[46] developed a strategy to construct 3D porphyrin-POMs coordination polymers that embedded POMs into the porphyrinic coordination polymer frameworks. Hydrothermal reaction of MoO_3, copper nitrate and TPyP in water at 200 °C afforded a 3D hybrid of $[Cu(TPyP)Cu_2Mo_3O_{11}]$. Its structure consists of a tessellated porphyrin network linked through bimetallic $\{Cu_2Mo_3O_{11}\}$ oxide chains into a covalently connected 3D framework. From a similar reaction, $[\{Fe(TPyP)\}_3Fe(Mo_6O_{19})_2]\cdot xH_2O$ was obtained, and it exhibited a 3D cationic framework of $[Fe_4(TPyP)_3]_n^{4n+}$ with entrained $\{Mo_6O_{19}\}^{2-}$ cluster anions (Fig. 17). The large cavities in these iron-porphyrin cubes are alternately populated by $\{Mo_6O_{19}\}^{2-}$ clusters and diffused with disordered water molecules. These two structures illustrated the synergistic interaction of the various structural components and that molybdenum oxide structures may be readily modified by the porphyrin building blocks as well as the porphyrin ligated metal atoms.

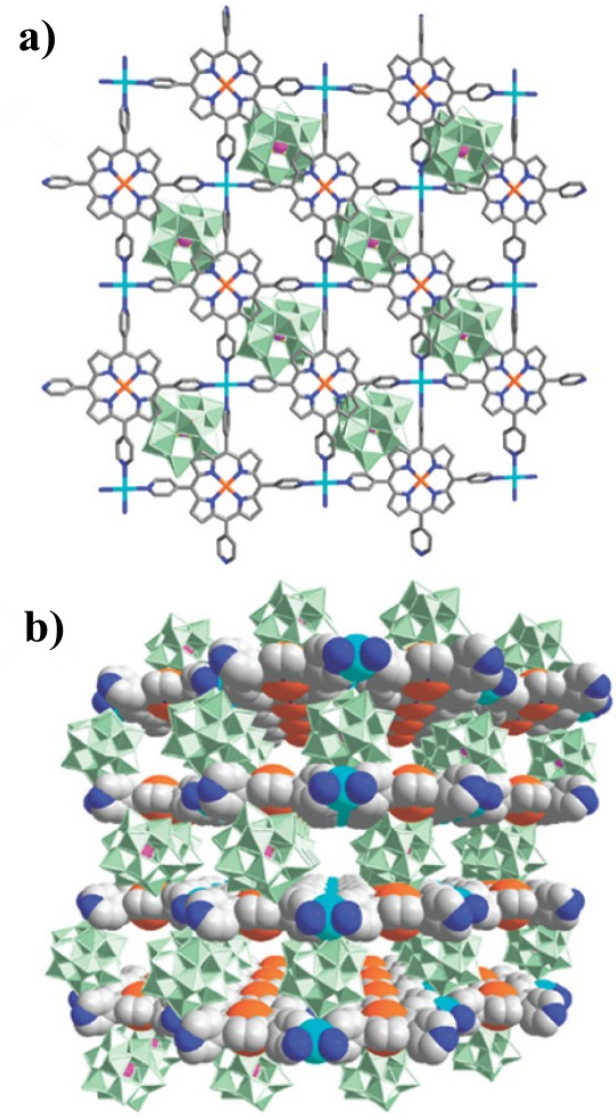

Figure 18. (a) Arrangement of a single layer of the lamellar framework of $[Cd(DMF)_2Mn^{III}(DMF)_2TPyP]_n^{3n+}$ and a layer of the $[PW_{12}O_{40}]^{3-}$ polyanions, as viewed along the *c* axis. (b) Perspective view of the packing diagram of the hybrid material along the [110] direction. Color scheme: Mn^{III}, orange; Cd, cyan; $\{WO_6\}$, green octahedra; P, purple; N, blue; C, gray. DMF molecules and H atoms have been omitted for clarity. (Reproduced from ref. 47 with permission, copyright 2012 American Chemical Society.)

The synthesis of metalloporphyrin-POM-based hybrids is extremely difficult, due to the adverse solubility of POMs and porphyrins (soluble in water and organic solvents, respectively). To overcome this difficulty, the Chuande Wu group developed a two-step synthesis strategy.[47] A reaction of $H_3PW_{12}O_{40}$ with Mn^{III}Cl-TPyP in DMF was first carried out to form the zwitterionic complex $\{[Mn^{III}(DMF)_2TPyP](PW_{12}O_{40})\}^{2-}$. The combined components could be readily dissolved both in water and organic solvents (e.g., DMF, MeOH, etc.). Thus, $\{[Cd(DMF)_2Mn^{III}(DMF)_2TPyP](PW_{12}O_{40})\}\cdot 2DMF\cdot 5H_2O$ was successfully isolated upon reaction of the zwitterionic complex

and $Cd(NO_3)_2{\cdot}4H_2O$. Its structure is composed of alternate layers of POM anions and porphyrin-containing cationic nets as dipicted in Fig. 18. Interestingly, the hybrid material exhibits good capability for scavenging of dyes and heterogeneous oxidation of alkylbenzenes with high yields and 100% selectivity.

Strategy 4: Encapsulation of porphyrins into the cages and post-synthetic modification

Porous metal-organic materials (MOMs) that incorporate reactive species such as metalloporphyrins, have drawn increasing attention[48] because they can demonstrate the physicochemical properties of the metalloporphyrins and their applications as catalysts and dyes while retaining permanent porosity. Such MOMs constructed by selective encapsulation of porphyrins into the cages or post-synthetic modification can facilitate gas storage,[49, 50] separations,[33] and catalysis.[51] In some cases, post-synthetic modification may afford target structures that can not be obtained by direct reaction of the metal ions with the ligands. In addition, this approach also provides the possibility to immobilize the metalloporphyrins in solid matrices where the macrocycles can be isolated and their catalytic sites are protected, in order to prohibit the self-dimerization and oxidative degradation.[52]

The Zaworotko group[53] reported that reaction of biphenyl-3,4',5-tricarboxylate (H_3BPT), $CdCl_2$ and TMPyP (TMPyP=meso-tetra(N-methyl-4-pyridyl)porphine tetratosylate) afforded porph@MOM-10 (Fig. 19), which contains Cd-TMPyP cations encapsulated in an anionic Cd(II) carboxylate framework. Thus, TMPyP acts as a template for the generation of porph@MOM-10, which can undergo post-synthetic modification by Mn(II) or

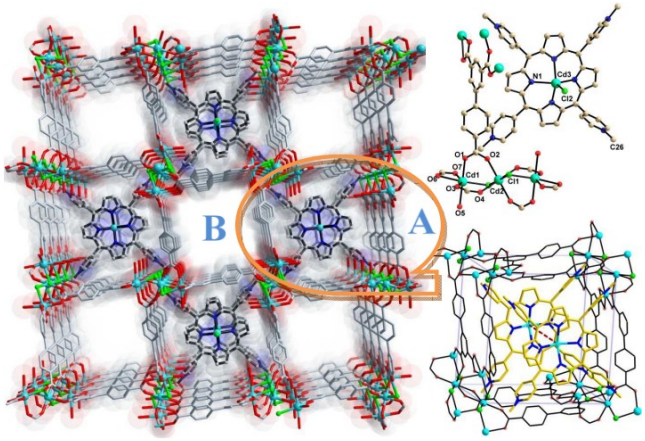

Figure 19. (Left) Projection of the structure of porph@MOM-10 along the *c* axis; (above right) the components of the framework and CdTMPyP cations in porph@MOM-10; (below right) an illustration of CdTMPyP cations trapped in the cuboid boxes of porph@MOM-10. (Reproduced from ref. 53 with permission, copyright 2012 American Chemical Society.)

Table 1: Structural details of the crystal structure of porph@MOM-11 and its PSM derivatives.[a]

	Porph@MOM-11	porph(Cl^-)@MOM-11-(Na^+)	porph(Cl^-)@MOM-11-(Ba^{2+})	porph(Cl^-)@MOM-11-(Mn^{2+})	porph(Cl^-)@MOM-11 (Cd^{2+})
Site occupancy[b]		Na 0.5	Ba 0.25	Mn 0.5	Cd 1
MBBs[c]	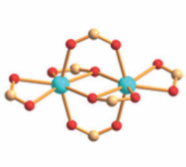	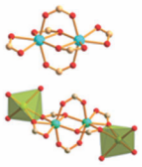	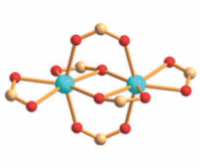	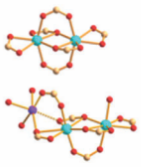	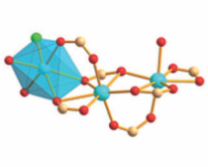
MBBs[c]	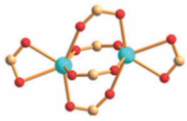	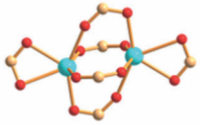	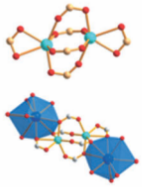	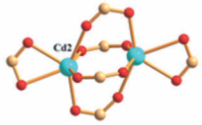	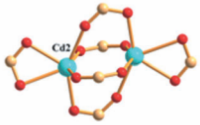
Porphyrins	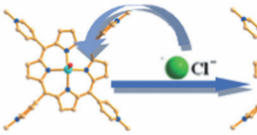	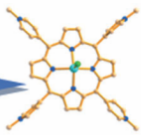	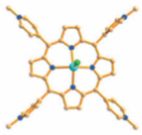	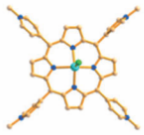	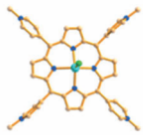
Channels incorporating metal cations	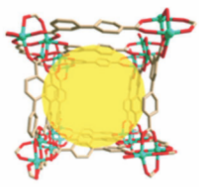	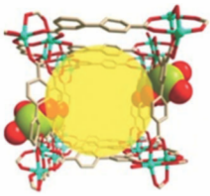	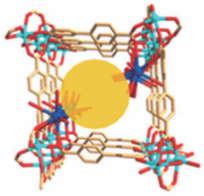	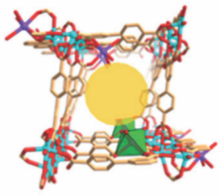	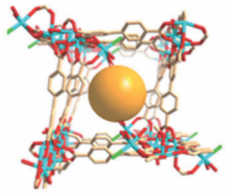

[a] Cd (turquoise), Cl (green), Mn (pink), Na (lime), Ba (indigo). [b] Incorporated metals. [c] Cd1 is the right Cd atom, Cd2 the left Cd atom. (Reproduced from ref. 54 with permission, copyright 2012 John Wiley and Sons.)

Cu(II) *via* single-crystal to single-crystal transformation processes. Thus, crystals of porph@MOM-10 were immersed in a methanol solution of $MnCl_2$, and monitored by UV-Vis spectroscopy, indicating that the conversion of Cd-TMPyP to Mn-TMPyP was complete within one week. Atomic Absorption revealed that the Cd-framework was almost completely exchanged by Mn after one month. When immersed in a solution of $CuCl_2$, Cd-TMPyP (λ_{max} = 426.4 nm) was transformed to Cu-TMPyP (λ_{max} = 430.0 nm) but the Cd-framework was only partly exchanged with Cu. The resulting Mn- and Cu-exchanged variants exhibit catalytic activity for epoxidation of trans-stilbene. Reaction of H_3BPT, $Cd(NO_3)_2{\cdot}4H_2O$, and TMPyP in DMF/H_2O yielded a dark green prismatic crystal, porph@MOM-11,[54] whose structure is an anionic framework encapsulating cationic porphyrins in alternating channels. Porph@MOM-11 enabled the post-synthetic modification involving single-crystal to single-crystal transformation processes induced by the addition of metal salts. When it was immersed in a solution of NaCl, $BaCl_2$, $MnCl_2$, or $CdCl_2$ respectively for several days, the framework Cd would be partially exchanged by these added metal cations to afford various derivatives (Table 1). The stoichiometric incorporation of the salts allowed a systematic study of the effect of metal cations upon gas adsorption. These derivatives exhibit higher selectivity for CO_2 versus CH_4 compared with the parent porph@MOM-11. When immersed in 0.05 M $Cu(NO_3)_2$ in MeOH for 10 days, porph@MOM-11 (P11) also undergoes a single-crystal to single-crystal transformation with its dimetallic $[Cd_2(COO)_6]^{2-}$ units converted into a larger, novel tetrametallic $[Cu_4X_2(COO)_6(S)_2]$ (S =MeOH, H_2O; X = CH_3O^-, OH^-), affording P11-Cu with increased unit cell size, pore size, and surface area.[55] The direct reaction of Cu salts with H_3BPT did not afford P11-Cu. The use of mixed metal salt solutions (Cd^{2+}/Cu^{2+}) with varying ratios enabled a systematic study of the metal exchange process in P11. When the Cd^{2+}/Cu^{2+} ratio was 2:1, the Cd^{2+} ions both in the framework and the porphyrin cores were fully exchanged with Cu^{2+}. However, when Cd^{2+}/Cu^{2+} ratios were increased to 4:1 or 8:1, the Cd^{2+} in the framework were only partially exchanged and

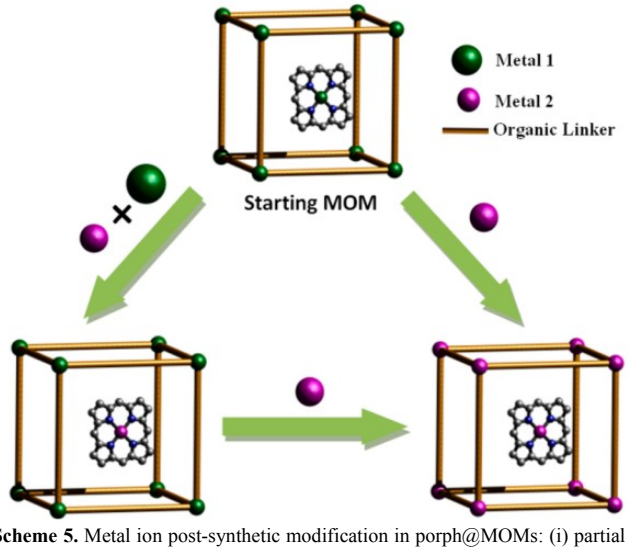

Scheme 5. Metal ion post-synthetic modification in porph@MOMs: (i) partial exchanged with Metal 2 in the presence of both Metal 1 and 2 (bottom left); (ii) complete exchange with Metal 2 (bottom right). (Reproduced from ref. 55 with permission, copyright 2013 American Chemical Society.)

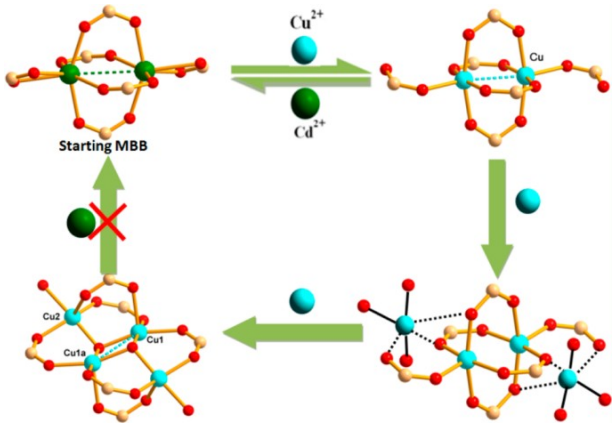

Scheme 6. Possible pathway to $[Cu_4X_2(COO)_6(S)_2]$ starting from $[Cd_2(COO)_6]^{2-}$ as determined by Metal Ion Exchange and SCXRD. (Reproduced from ref. 55 with permission, copyright 2013 American Chemical Society.)

the Cd^{2+} ions in the porphyrin cores were fully exchanged with Cu^{2+}. When the Cd^{2+}/Cu^{2+} ratio was 16/1, the framework Cd^{2+} cations were totally retained and Cd^{2+} in the encapsulated porphyrins were completely exchanged. These processes are summarized in Scheme 5. And Scheme 6 shows how porph@MOMs might undergo the metal exchange in the framework.

Conclusions

In this highlight, we briefly summarized recent advances in the synthesis, functionalization, and applications of PCPs. We have described several crystal-engineering strategies that can be successfully applied in the construction of extended PCPs: i) introducing novel multimetal nodes like the lanthanides and Zr_6 cluster, or inserting active metal ions into the porphyrin core; ii) design and synthesize new porphyrinic ligands with multi-carboxyl or pyridyl coordination sites; iii) combination with inorganic polyoxometalates; iv) encapsulating of porphyrins into cages and post-synthetic modification. In conclusion, porphyrin-based coordination polymers will definitely receive increasing attention due to their diverse and attractive structures in addition to their interesting properties in various areas, especially in heterogeneous catalysis, gas storage, and separation.

Acknowledgements

This work was financially supported by NSFC (91227201), the Program for Professor of Special Appointment (Eastern Scholar) at Shanghai Institutions of Higher Learning, Program for New Century Excellent Talents in University (NCET-11-0638), and the Fundamental Research Funds for the Central Universities (WK1013002).

References

1. (a) J. P. Zhang, X. C. Huang, X. M. Chen, *Chem. Soc. Rev.*, 2009, **38**, 2385-2396; (b) O. M. Yaghi, M. O'Keeffe, N. W. Ockwig, H. K. Chae, M. Eddaoudi, J. Kim, *Nature*, 2003, **423**, 705; (c) J. Lee, O. K. Farha, J. Roberts, K. A. Scheidt, S. T. Nguyen, J. T. Hupp, *Chem. Soc. Rev.*, 2009, **38**, 1450–1459; (d) A. M. Spokoyny, D. Kim, A. Sumrein, C. A. Mirkin, *Chem. Soc. Rev.*, 2009, **38**, 1218-1227; (e) J. R. Long, O. M. Yaghi, *Chem. Soc. Rev.*, 2009, **38**, 1213-1214; (f) C.

X. Ding, J. Ni, Y. H. Yang, S. W. Ng, B. W. Wang, Y. S. Xie, *CrystEngComm*, 2012, **14**, 7312. (g) Y. S. Xie, J. Ni, F. K. Zheng, Y. Cui, Q. G. Wang, S. W. Ng, W. Zhu, *Cryst. Growth Des.* 2009, **9**, 118. (h) Y. Y. Tang, C. X. Ding, S. W. Ng, Y. S. Xie, *RSC Adv.* 2013, **3**, 18134. (i) T. Yamada, K. Otsubo, R. Makiura, H. Kitagawa, *Chem. Soc. Rev.*, 2013, **42**, 6655-6669.

2. (a) T. Uemura, N. Yanai, S. Kitagawa, *Chem. Soc. Rev.*, 2009, **38**, 1228-1236; (b) F. H. Zeng, J. Ni, Q. G. Wang, Y. B. Ding, S. W. Ng, W. H. Zhu, Y. S. Xie, *Cryst. Growth Des.* 2010, **10**, 1611. (c) C. Ding, X. Li, Y. Ding, X. Li, S. W. Ng, Y. Xie, *Cryst. Growth Des.* 2012, **12**, 3465; (d) J. Heine, K. M. Buschbaum, *Chem. Soc. Rev.*, 2013, **42**, 9232-9242; (e) C. Ding, X. Rui, C. Wang, Y. S. Xie, *CrystEngComm*, 2014,**16**, 1010-1019; (f) C. Ding, C. Gao, S. Ng, B. Wang, Y. S. Xie, *Chem. Eur. J.,* 2013, **19**, 9961-9972.
3. S. H. Cho, B. Ma, S. T. Nguyen, J. T. Hupp and T. E. Albrecht Schmitt, *Chem. Commun.*, 2006, 2563.
4. J. L. C. Rowsell and O. M. Yaghi, *Angew. Chem., Int. Ed.*, 2005, **44**, 4670.
5. Y. S. Bae, O. K. Farha, A. M. Spokoyny, C. A. Mirkin, J. T. Hupp and R. Q. Snurr, *Chem. Commun.*, 2008, 4135.
6. P. Horcajada, C. Serre, M. Vallet-Regí, M. Sebban, F. Taulelle and G. Férey, *Angew. Chem., Int. Ed.*, 2006, **45**, 5974.
7. (a) W. Q. Kan, J. Yang, Y. Y. Liu and J. F. Ma, *CrystEngComm*, 2012, **14**, 6271. (b) J. C. Hierso, R. Smaliy, R. Amardeila and P. Meuniera, *Chem. Soc. Rev.*, 2007, **36**, 1754.
8. (a) T. K. Chandrashekar, S. Venkatraman, *Acc. Chem. Res.*, 2003, **36**, 676; (b) E. Rose, A. Lecas, M. Quelquejeu, A. Kossanyi and B. Boitrel, *Coord. Chem. Rev.*, 1998, **178**, 1407; (c) M. O. Senge, J. Richter, *J. Porphyrins Phthalocyanines,* 2004, **8**, 934; (d) Y. S. Xie, J. P. Hill, A. L. Schumacher, Atula S. D. Sandanayaka, Y. Araki, P. A. Karr, J. Labuta, F. D'Souza, O. Ito, C. E. Anson, A. K. Powell, K. Ariga, *J. Phys. Chem. C,* 2008, **112**, 10559.
9. (a) M. E. Kosal and K. S. Suslick, *J. Solid State Chem.*, 2000, **152**, 87; (b) F. Scandola, C. Chiorboli, A. Prodi, E. Iengo and E. Alessio, *Coord. Chem. Rev.*, 2006, **250**, 1471.
10. E. Y. Choi, C. A. Wray, C. Hu, W. Choe, *CrystEngComm.* 2009, **11**, 553.
11. M. E. Kosal, J. H. Chou, S. R. Wilson, K. S. Suslick, *Nat. Mater.* 2002, **1**, 118.
12. H. J. Son, S. Jin, S. Patwardhan, S. J. Wezenberg, N. C. Jeong, M. So, C. E. Wilmer, A. A. Sarjeant, G. C. Schatz, R. Q. Snurr, O. K. Farha, G. P. Wiederrecht, J. T. Hupp, *J. Am. Chem. Soc.* 2013, **135**, 862.
13. (a) O. K. Farha, A. M. Shultz, A. A. Sarjeant, S. T. Nguyen, J. T. Hupp, *J. Am. Chem. Soc.* 2011, **133**, 5652; (b) R. W. Larsen, L. Wojtas, J. Perman, R. L. Musselman, M. J. Zaworotko, C. M. Vetromile, *J. Am. Chem. Soc.* 2011, **133**, 10356; (c) D. H. Lee, S. Kim, M. Y. Hyun, J. Y. Hong, S. Huh, C. Kim, S. J. Lee, *Chem. Commun.* 2012, **48**, 5512.
14. (a) H. Krupitsky, Z. Stein, I. Goldberg, C. E. Strouse, *J. Incl. Phenom.*, 1994, **18**, 177-192; (b) P. Dastidar, Z. Stein, I. Goldberg, C. E. Strouse, *Supramol. Chem.*, 1996, **7**, 257–270.
15. (a) I. Goldberg, *CrystEngComm*, 2002, **4**, 109-116; (b) I. Goldberg, *Chem. Commun.*, 2005, 1243-1254; (c) N. Zheng, J. Zhang, X. Bu, P. Feng, *Cryst. Growth Des.* 2007, **7**, 2576; (d) I. Goldberg, *CrystEngComm*, 2008, **10**, 637-645; (e) R. W. Seidel, R. Goddard, K. Föcker and I. M. Oppel, *CrystEngComm*, 2010, **12**, 387-394; (f) R. W. Seidel, I. M. Oppel, *CrystEngComm*, 2010, **12**, 1051-1053.
16. F. H. Allen, *The Cambridge Structural Database*, *Acta Crystallogr.* 2002, **B58**, 380-388.
17. S. George, S. Lipstman, and I. Goldberg, *Cryst. Growth Des.*, 2006, **12**, 2651.
18. (a) H. L. Jiang, D. Feng, J. R. Li, T. F. Liu, H. C. Zhou, *J. Am. Chem. Soc.* 2012, **134**, 14690; (b) A. Schaate, P. Roy, A. Godt, J. Lippke, F. Waltz, Wiebcke, M. P. Behrens, *Chem. Eur. J.* 2011, **17**, 6643.
19. M. Kim, S. M. Cohen, *CrystEngComm*, 2012, **14**, 4096-4104.
20. D. Feng, Z. Y. Gu, J. R. Li, H. L. Jiang, Z. Wei, and H. C. Zhou, *Angew. Chem., Int. Ed.* 2012, **124**, 10453-10456.
21. J. An, O. K. Farha, J. T. Hupp, E. Pohl, J. I. Yeh, N. L. Rosi, *Nat. Commun*. 2012, **3**, 604.
22. H. Deng, S. Grunder, K. E. Cordova, C. Valente, H. Furukawa, M. Hmadeh, F. Gandara, A. C. Whalley, Z. Liu, S. Asahina, H. Kazumori, M. O'Keeffe, O. Terasaki, J. F. Stoddart, O. M. Yaghi, *Science*, 2012, **336**, 1018-1023.
23. H. L. Jiang, D. Feng, K. Wang, Z. Y. Gu, Z. Wei, Y. P. Chen, and H. C. Zhou, *J. Am. Chem. Soc.* 2013, **135**, 13934−13938.
24. D. Feng, W. C. Chung, Z. Wei, Z. Y. Gu, H. L. Jiang, Y. P. Chen, D. J. Darensbourg, H. C. Zhou, *J. Am. Chem. Soc.,* **2013**, 135, 17105-17110.
25. J. H. Cavka, S. Jakobsen, U. Olsbye, N. Guillou, C. Lamberti, S. Bordiga, K. P. Lillerud, *J. Am. Chem. Soc.*, 2008, **130**, 13850-13851.
26. M. H. Xie, X. L. Yang, C. D. Wu, *Chem. Commun.*, 2011, **47**, 5521.
27. (a) X. Q. Yu, J. S. Huang, W. Y. Yu, C. M. Che, *J. Am. Chem. Soc.* 2000, **122**, 5337; (b) S. M. Ribeiro, A. C. Serra, A. M. Gonsalves, *Tetrahedron*, 2007, **63**, 7885.
28. M. H. Xie, X. L. Yang, C. Zou, C. D. Wu, *Inorg. Chem*. 2011, **50**, 5318-5320.
29. R. Patra, H. M. Titi, I. Goldberg, *Cryst. Growth Des*. 2013, **13**, 1342.
30. S. Lipstman, I. Goldberg, *Cryst. Growth Des.* 2013, **13**, 942.
31. E. Y. Choi, L. D. DeVries, R. W. Novotny, C. Hu, W. Choe, *Cryst. Growth Des.* 2010, **10**,171.
32. S. Lipstman, I. Goldberg, *Cryst. Growth Des.* 2010, **10**, 5001.
33. X. S. Wang, L. Meng, Q. Cheng, C. Kim, L. Wojtas, M. Chrzanowski, Y. S. Chen, X. P. Zhang, S. Ma, *J. Am. Chem. Soc.* 2011, **133**, 16322–16325.
34. S. Matsunaga, N. Endo, W. Mori, *Eur. J. Inorg. Chem.* 2012, 4885.
35. L. Meng, Q. Cheng, C. Kim, W. Y. Gao, L. Wojtas, Y. S. Chen, M. J. Zaworotko, X. P. Zhang, S. Ma, *Angew. Chem. Int. Ed*. 2012, **51**, 10082-10085.
36. X. L. Yang, M. H. Xie, C. Zou, Y. He, B. Chen, M. O' Keeffe, C. D. Wu, *J. Am. Chem. Soc.* 2012, **134**, 10638-10645.
37. X. S. Wang, M. Chrzanowski, C. Kim, W. Y. Gao, L. Wojtas, Y. S. Chen, X. P. Zhang, S. Ma, *Chem. Commun.*, 2012, **48**, 7173–7175.
38. J. J. Perry, J. A. Perman, M. J. Zaworotko, *Chem. Soc. Rev.*, 2009, **38**, 1400-1417.
39. X. S. Wang, M. Chrzanowski, W. Y. Gao, L. Wojtas, Y. S. Chen, M. J. Zaworotko, S. Ma, *Chem. Sci.*, 2012, **3**, 2823.
40. X. S. Wang, M. Chrzanowski, L. Wojtas, Y. S. Chen, S. Ma, *Chem. Eur. J.* 2013, **19**, 3297 – 3301.
41. J. A. Johnson, Q. Lin, L. C. Wu, N. Obaidi, Z. L. Olson, T. C. Reeson, Y. S. Chen and J. Zhang, *Chem. Commun.*, 2013, **49**, 2828.
42. Q. Zha, C. Ding, X. Rui, Y. S. Xie, *Cryst. Growth Des.* 2013, **13**, 4583.
43. (a) P. Kogerler, L. Cronin, *Angew. Chem., Int. Ed*. 2005, **44**, 844. (c) A. Dolbecq, E. Dumas, C. R. Mayer, P. Mialane, *Chem. Rev.* 2010, **110**, 6009; (b) J. X. Meng, Y. Lu, Y. G. Li, H. Fu, E. B. Wang, *Cryst.Growth Des.* 2009, **9**, 4116.
44. (a) R. Yu, X. F. Kuang, X. Y. Wu, C. Z. Lu, J. P. Donahue, *Coord. Chem. Rev.*, 2009, **253**, 2872; (b) U. Kortz, A. Müller, J. van Slageren, J. Schnak, N. S. Dalal, M. Dressel, *Coord. Chem. Rev.*, 2009, **253**, 2315;
45. (a) M. D. McGehee, A. J. Heeger, *Adv. Mater.* 2000, **12**, 1655; (b)H. E. Katz, Z. Bao, S. L. Gilat, *Acc. Chem. Res.* 2001, **30**, 359; (c) S. Pramanik, C. Zheng, T. J. Emge, J. Li, *J. Am. Chem. Soc.*, 2011, **133**, 4153; (d) A. Lan, K. Li, H. Wu, D. H. Olson, T. J. Emge, W. Ki, M. Hong, J. Li, *Angew. Chem. Int. Ed.*, 2009, **48**, 2334.
46. D. Hagrman, P. J. Hagrman, J. Zubieta, *Angew. Chem. Int. Ed.* 1999, **38**, 3165.
47. C. Zou, Z. Zhang, X. Xu, Q. Gong, J. Li and C. D. Wu, *J. Am. Chem. Soc.*, 2012, **134**, 87.
48. M. H. Alkordi, Y. Liu, R. W. Larsen, J. F. Eubank, M. Eddaoudi, *J. Am. Chem. Soc.*, 2008, **130**, 12639.
49. E. Y. Choi,; C. A. Wray, C. Hu, W. Choe, *CrystEngComm*, 2009, **11**, 553;
50. A. M. Shultz, O. K. Farha, J. T. Hupp, S. T. Nguyen, *J. Am. Chem. Soc.* 2009, **131**, 4204.
51. C. Y. Lee, O. K. Farha, B. J. Hong, A. A. Sarjeant, S. T. Nguyen, J. T. Hupp, *J. Am. Chem. Soc.* 2011, **133**, 15858.
52. C. Guo, J. Song, X. Chen, G. J. Jiang, *Mol. Catal. A.* 2000, 157, 31-40.
53. Z. Zhang, L. Zhang, L. Wojtas, P. Nugent, M. Eddaoudi, M. J.

Zaworotko, *J. Am. Chem. Soc*. 2012, **134**, 924.
54. Z. Zhang, W. Gao, L. Wojtas, S. Ma, M. Eddaoudi, and M. J. Zaworotko, *Angew. Chem. Int. Ed.*, 2012, **124**, 9464.
55. Z. Zhang, L. Wojtas, M. Eddaoudi, M. J. Zaworotko, *J. Am. Chem. Soc*. 2013, **135**, 5982.

For Table of Contents Entry Use Only

Recent Advances in the Design Strategies for Porphyrin-based Coordination Polymers

Quanzheng Zha, Xing Rui, Tiantian Wei and Yongshu Xie

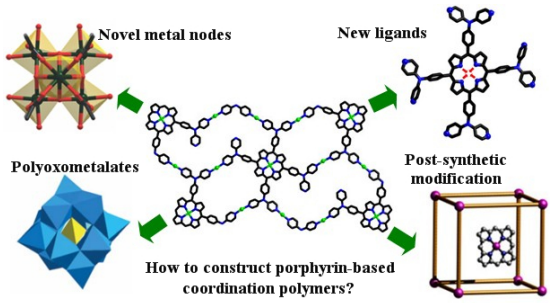

Strategies to construct the porphyrin-based coordination polymers are summarized based on metal nodes, porphyrin ligands, inorganic polyoxometalates and post-synthetic modification.